ELSEVIER

Earth and Planetary Science Letters 201 (2002) 337–352

EPSL

www.elsevier.com/locate/epsl

Melt viscosity, temperature and transport processes, Troodos ophiolite, Cyprus

Hans Schouten *, Peter B. Kelemen

Department of Geology and Geophysics, Woods Hole Oceanographic Institution, MS#24, Woods Hole, MA 02543-1541, USA

Received 27 November 2000; received in revised form 22 March 2002; accepted 3 May 2002

Abstract

The lava section in the Troodos ophiolite, Cyprus, is chemically stratified and divided into a shallow lava sequence with low TiO_2 content and a deeper lava sequence with high TiO_2 content. We calculate the viscosity at magmatic temperature based on major element chemistry of lavas in Cyprus Crustal Study Project (CCSP) Holes CY-1 and 1A. We find that typical shallow low-Ti lavas have a magmatic viscosity that is two to three orders of magnitude lower than that of the deeper high-Ti lavas. This implies that, after eruption on-axis, Troodos low-Ti lavas would have been able to flow down the same slope faster and farther than high-Ti lavas. The calculated lava viscosity increases systematically from the lava–sediment interface to the bottom of the composite Hole CY-1/1A. This suggests that an efficient process of lava segregation by viscosity on the upper flanks of the paleo Troodos rise may have been responsible for the chemical stratification in the Troodos lava pile. Calculated magmatic temperature and molar Mg/(Mg+Fe), or Mg#, decrease systematically down-section, while SiO_2 content increases. Correlation of Mg# in the lavas with Mg# in the underlying, lower crustal plutonic rocks sampled by CCSP Hole CY-4 shows that the shallow lavas came from a high-temperature, lower crustal magma reservoir which is now represented by high-Mg# pyroxenite cumulates, while the deeper lavas were erupted from a lower-temperature, mid-crustal reservoir which is now represented by gabbroic cumulates with lower Mg#.

Keywords: magmas; viscosity; lava flows; mid-ocean ridges; Troodos Ophiolite; Cyprus

1. Introduction

The Late Cretaceous Troodos ophiolite is one of the best studied in the world. It has a unique advantage of several drill holes penetrating most of the crustal sequence, composed of a plutonic complex, stratigraphically overlain successively by a sheeted dike complex, extrusive sequences and pelagic sediments (Fig. 1). The ophiolite complex forms a gentle anticline with an approximately EW axis due to uplift and doming during emplacement. On its northern flank the complex dips gently north, which is where Cyprus Crustal Study Project (CCSP) Holes CY-1/1A and CY-2/2A sampled most of the extrusive section. Hole CY-4, located ca 15 km closer to the axis of the anticline, S of the village of Palekhori, started near the base of the sheeted dikes and sampled more than 2000 m of the plutonic section.

* Corresponding author. Tel.: +1-508-289-2574; Fax: +1-508-457-2150.
E-mail address: hschouten@whoi.edu (H. Schouten).

0012-821X/02/$ – see front matter © 2002 Published by Elsevier Science B.V.
PII: S0012-821X(02)00709-4

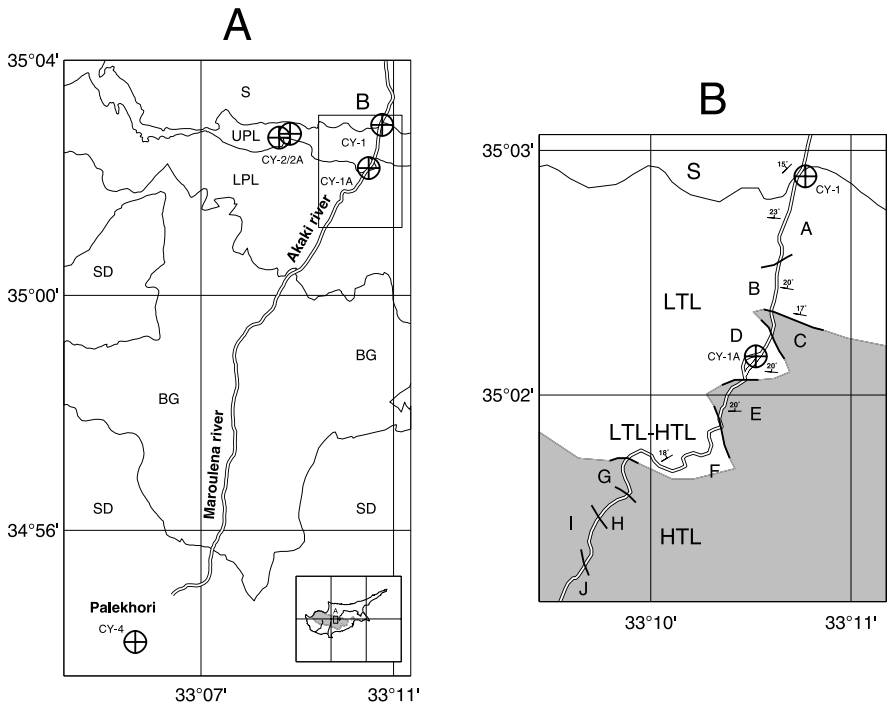

Fig. 1. (A) Location map for B (box) and the CCSP drill holes (crossed circles) that sampled most of the crustal section of the ophiolite. S – sediments; UPL – Upper Pillow Lavas; LPL – Lower Pillow Lavas; BG – Basal Group; SD – sheeted dikes. Insert shows island of Cyprus and location of A (box) on the northern flank of the Troodos ophiolite (shaded). (B) Generalized geologic map of the Akaki River canyon showing location of Holes CY-1 and CY-1A. Volcanic units A–J are after [47]. Alternating chemistry of the units [47,48] shows a zone of alternating high-Ti and low-Ti lava units, sandwiched between the shallow low-Ti lavas to the north and deeper high-Ti lavas (shaded) to the south. Solid line segments – contacts between lava units mapped along the Akaki River [47,48]. These are interpreted to fit a saw-toothed boundary that indicates a limited and infrequent inter-fingering of high- and low-Ti lavas, similar to that observed in the HTL–LTL transition zone in Hole CY-1A (see Fig. 2B). Dips of lava flow surfaces [22,49,50] reflect the gentle northward dip of the ophiolite.

Early workers (e.g. [1]) divided the Troodos extrusives into Upper Pillow Lavas, Lower Pillow Lavas and the Basal Group. The divisions were based on mineralogy, color (alteration), and the abundance of dikes. An olivine phyric group at the top of the sequence constitutes the Upper Pillow Lavas resting on generally aphyric Lower Pillow Lavas. In the Upper Pillow Lava sequence, dike abundance is only a few percent of total outcrop, in the Lower Pillow Lava sequence it is 30–50%, and in the Basal Group the dike abundance is 80–90% [1]. The width of the boundary between sequences is highly variable. In most localities, the boundary between Upper and Lower Pillow Lavas is transitional or poorly defined; in others it is placed at an angular unconformity or thin layers of intercalated, ochreous sediments or hematitic shales [1–3]. The extrusive section of the Troodos ophiolite grades downwards into the sheeted dike complex through a zone of intermixed dikes and pillow screens known as the Basal Group. A greater abundance of dikes and higher degree of tectonic deformation and dissection units mark this zone as compared to the overlying lava series. The dikes in the Basal Group are sinuous, with 10–20% pillow screens. The dikes in the underlying sheeted dike complex are planar with no identifiable pillow screens (dike abundance $>95\%$). The transition from Basal Group to sheeted dike complex is typically less than 100 m [4].

On the basis of studies of the alteration and

metamorphism of the Troodos lavas, Gass and Smewing [4] and Smewing et al. [5] modified this early subdivision and defined an axis sequence and an off-axis sequence (but not far enough off-axis for a sedimentary sequence to develop). The boundary between the two sequences was based on a relative lack of secondary mineralization in the younger, off-axis sequence. Subsequent alteration studies [6–8] suggest that this interpretation was incomplete and based on erroneous data [9].

Studies of volcanic glasses [6] occurring throughout the volcanic sequence allowed the division of the volcanic pile into a shallow picrite–basalt–basaltic andesite assemblage with low TiO_2 concentration, and a deeper basalt–andesite–dacite–rhyodacite assemblage with high TiO_2 content (>0.85 wt% [10]). The shallow lava sequence consists of highly depleted magmas of 'boninitic' affinity. Less depleted, tholeiitic basalts and their derivatives dominate the deeper lava sequence. In a few cases (e.g. [11]) these low- and high-Ti suites correspond to the Upper and Lower Pillow Lavas as defined by Bear [1], but elsewhere the stratigraphic relations are less clear due to incomplete sampling, structural complexity and poor field exposures [12]. The two suites were considered genetically independent because they appeared to be unrelated by fractional crystallization processes [6].

Most published data support the notion that the low-Ti lavas were erupted after the high-Ti lavas; however, some areas show either the opposite relationship or a complex stratigraphy (e.g. [11,13–15]). The thickness of the upper low-Ti unit is also highly variable. For example, in Holes CY-2/2A, the low-Ti suite is <100 m whereas it is >400 m in Hole CY-1/1A. Moreover, low-Ti lavas comprise on average one third of the volcanic sequence [13] whereas in the Akaki area it comprises two thirds.

Analyses of the rocks from Holes CY-1 and CY-1A support the proposed division of the volcanic sequence into a younger low-Ti lava suite overlying an older high-Ti suite, separated by a transition zone of mixed TiO_2 concentrations (Fig. 2B). Studies of the Troodos sheeted dikes showed that chemically the dikes are a close match to the shallow and deeper pillow lava sequence and the high- and low-Ti series identified in the lava glasses [6]. The low-Ti suite in the sheeted complex comprises about 20% of the dikes, which show no preferred age relationship with respect to those of the high-Ti suite [10]. These results indicate that the low- and high-Ti lavas were co-magmatic and erupted penecontemporaneously from adjacent fissures on the spreading center axis. That the low- and high-Ti lavas erupted close together but were deposited separately without much overlap represents an apparent paradox [16].

In this paper we use a composite of the CCSP CY-1 and CY-1A drill cores to reconstruct the Troodos spreading center. Down-core chemistry and dike fraction provide evidence for a bimodal lava deposition environment at the Troodos spreading center. The drill core data suggest that the shallow, low-Ti lavas were deposited off-axis, outside the zone of dike injection, on top of the deeper high-Ti lavas, which were deposited on-axis inside the zone of dike injection.

To address the apparent paradox that low- and high-Ti lavas erupted close together but were deposited separately, we calculate physical properties based on major element chemistry of the Troodos lavas in the CY-1/1A drill core. It is found that high-viscosity lavas were deposited entirely within the on-axis zone of dike injection, while lower viscosity lavas flowed further and were deposited primarily in an off-axis setting. Thus, the stratigraphic sequence of lava compositions is probably explained by melt viscosity.

As will be shown later, data from the CY-1/1A volcanic rocks do not support the division of the lavas into two distinct, genetically unrelated suites, but instead suggest incomplete mixing of at least two magma series, combined with crystal fractionation, throughout the entire differentiation sequence. Thus, while Troodos lavas may be composed of mixtures of 'boninitic' and tholeiitic magma series, a sharp division between two distinct series cannot be made in the CY-1/1A lavas based on TiO_2 content alone. Instead, both magma series, and intermediate mixtures of the two, are represented by primitive (low TiO_2) and evolved (high TiO_2) lavas. We find that the

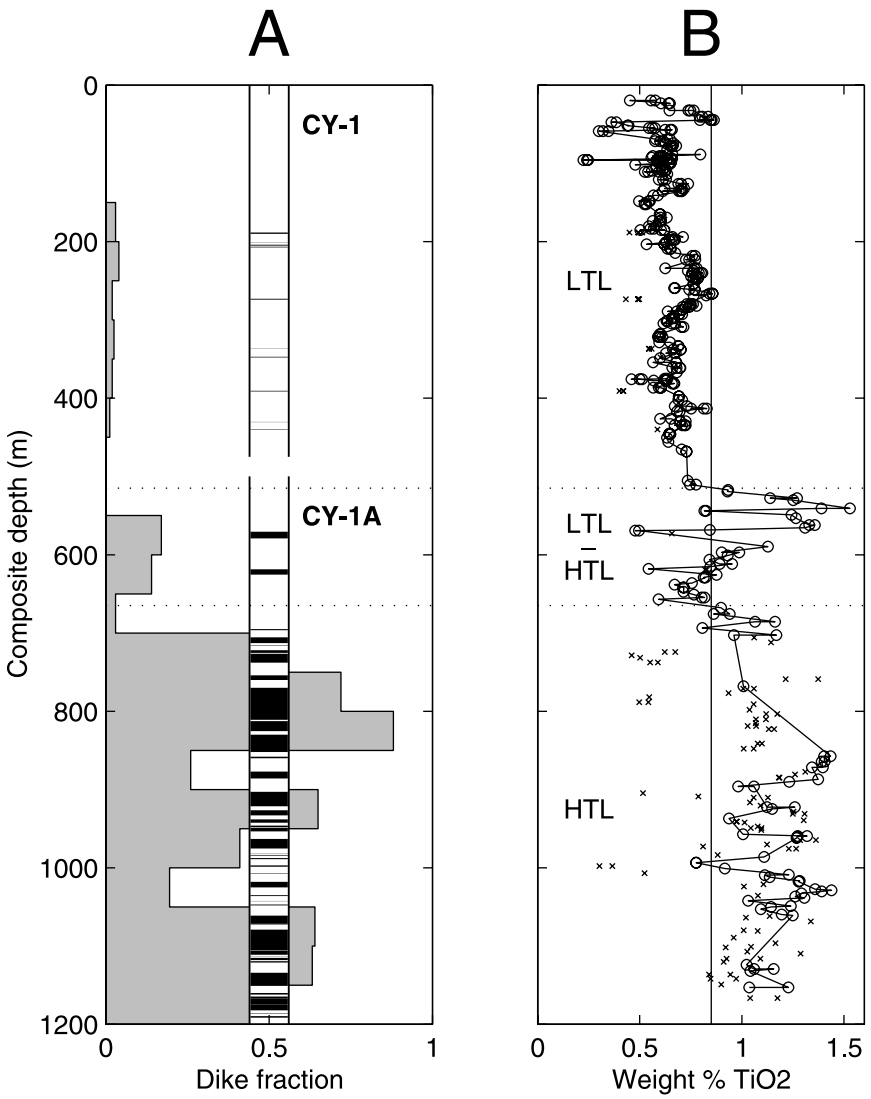

Fig. 2. Dike fraction and TiO_2 concentration in CCSP Holes CY-1 and CY-1A [17] plotted against composite depth. CY-1A is suspended beneath CY-1 starting at 500 m. (A) Dike distribution in core (center) from lithologic log of Malpas and Barnable [19] and 50 m core length averages of the dike fraction (shaded). (B) Anhydrous TiO_2 concentration based on Gibson et al. [17] (o's are lavas; x's are dikes). Thin line at 0.85 wt% separates low from high Ti concentrations [10]. Dotted lines at 515 and 665 m bound the transition zone from low-Ti lavas (LTL) above to high-Ti lavas (HTL) below. Dike fraction increases with depth in the sequence and closely follows the division based on TiO_2 content of the lavas, i.e. very few dikes ($<2\%$) in the low-Ti section, $11 \pm 7\%$ dikes in the chemical transition zone, and $53 \pm 21\%$ dikes in the high-Ti section.

primitive lavas were probably erupted from high-temperature magma reservoirs in the lower part of the plutonic crustal section, while the evolved lavas probably were derived from lower-temperature magma reservoirs near the top of the plutonic section.

2. CCSP Holes CY-1 and CY-1A

CCSP Holes CY-1 and CY-1A sampled an almost continuous stratigraphic section through the extrusive sequence and the transition into the sheeted dike complex of the Troodos ophiolite

[17]. Hole CY-1 was drilled at the lava–sediment contact in the Akaki River canyon (Fig. 1) and penetrated the upper 475 m of the section. CY-1A, located about 1 km south of CY-1 (Fig. 1), penetrated the lower lava section to a depth of 701 m. In the composite section (Fig. 2) the CY-1A section is suspended from a depth of 500 m, 25 m below the base of CY-1 [18].

We separate the CY-1/1A samples into extrusives (o's in Fig. 2B) and dikes (x's in Fig. 2B) using the lithologic log of Malpas and Barnable [19] (see central column in Fig. 2A). The extrusives of the CY-1/1A section can be divided into a shallow low-Ti suite (<0.85 wt%) and a deeper high-Ti suite (>0.85 wt%), separated by a transition zone of alternating low-Ti and high-Ti lava units (bracketed section at 515–665 m in Fig. 2B). Whereas the low-Ti suite (0–515 m) contains no high-Ti lava samples, the high-Ti portion of the core (>665 m) contains an occasional low-Ti lava sample.

The TiO_2 content of samples from dikes (x's in Fig. 2B) identifies dikes feeding the low-Ti lavas of the shallow section and those feeding the deeper high-Ti lavas. No high-Ti dikes are found crosscutting the low-Ti lavas of the shallow section. Low-Ti dikes are crosscutting the high-Ti lavas at all levels. In the high-Ti suite of lavas (>665 m), 20% of dike samples have low TiO_2 content. Dike fraction (Fig. 2A) increases with depth in the sequence and closely follows the division based on TiO_2 content of the lavas, i.e. very few dikes ($<2\%$) in the low-Ti section, $11\pm7\%$ dikes in the chemical transition zone, and $53\pm21\%$ dikes in the high-Ti section.

Field relations in the Akaki River canyon, where the CY-1 and CY-1A holes were drilled, show a transition zone of alternating low-Ti and high-Ti lava units, sandwiched between the shallower low-Ti lava series to the north and the deeper high-Ti lava series to the southeast (Fig. 1B). The mapped contacts between the lava units (solid lines in Fig. 1B) are interpreted here to be part of a saw-toothed boundary that would indicate limited and infrequent inter-fingering of high- and low-Ti lavas, similar to that observed in the transition zone in Hole CY-1/1A (bracketed section in Fig. 2B).

Schmincke and Bednarz [20] estimate that the total extrusive crust above the sheeted dikes on the northeastern flank of the Troodos is made up of between five and 10 individual volcanoes. They propose a general volcanic and structural evolution marked by a series of volcano-tectonic–hydrothermal cycles in which initial volcanic extension is followed by hydrothermal activity and subsequent extrusion and building of the volcanic edifice. They show that at typical magmatic temperatures of the Troodos low-Ti lavas have viscosities that are one to two orders of magnitude lower than that of the high-Ti lavas ([20], figure 26).

3. Lava deposition and dike injection in the Troodos paleo-spreading center, or, how far is far?

In a sequence of lava flows, the shallower sequence is deposited later than the deeper sequence. In a seafloor spreading environment like the Troodos spreading center, later deposition of lavas is equivalent to lava deposition farther from the spreading axis; earlier deposition is equivalent to deposition closer to the axis (e.g. [21]). From this it follows that the high-Ti lavas, restricted to the deeper part of the section (665–1200 m in Fig. 2B), were deposited closer to the spreading axis, while the low-Ti lavas, restricted to the shallower part of the section (0–515 m in Fig. 2B), were deposited farther from the axis. High- and low-Ti lavas inter-finger only in a relatively narrow transition zone (515–665 m in Fig. 2B). From the distribution of high- and low-Ti lavas in the cores we can conclude that high-Ti lavas were deposited nearest to the spreading axis; the bulk of the low-Ti lavas were deposited farther away outside the zone of high-Ti lava deposition with only a small amount of overlap between the two depocenters (Fig. 3).

The hypothesis of a spatial separation between the high- and low-Ti lava depocenters in the Troodos spreading center is further supported by observations of the abundance of dikes in the drill cores. The distribution of dikes and the dike fraction per unit core length in the CY-1/1A drill

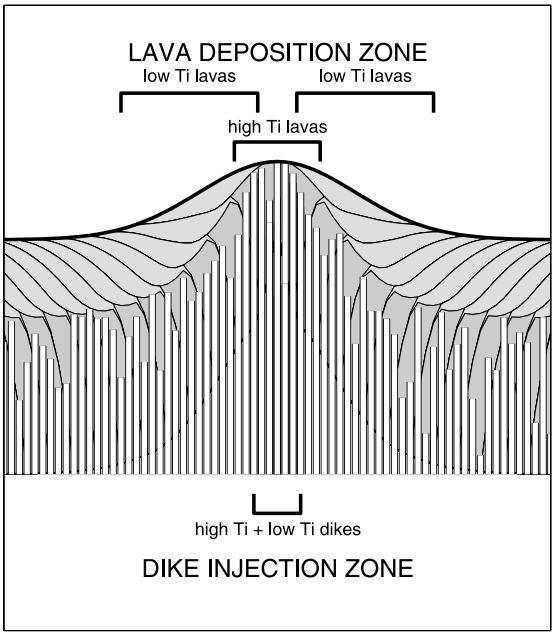

Fig. 3. Schematic geometry (not to scale) of lava deposition in the Troodos seafloor spreading center based on field observations and the CY-1/1A drill core. Horizontal brackets indicate the width of the neovolcanic zone consisting of high- and low-Ti lava depocenters and of the dike injection zone. Darker shading marks the deeper high-Ti lavas, and light shading marks the shallow low-Ti lavas. High-Ti lavas build a central volcanic ridge around the axial eruption center. Lower-viscosity, low-Ti lavas, which erupted from the same center, are efficiently drained away through lava tubes or channels to the flanks of the ridge. Episodic lateral growth of the central volcanic ridge causes high-Ti lava flows to overlap with low-Ti lavas on the flanks and generate the saw-toothed contact between high- and low-Ti series seen in the Akaki canyon (Fig. 1B) and in the CY-1/1A drill core (Fig. 2B). The lower high-Ti lavas are mostly deposited within the dike injection zone and therefore mostly riddled with dikes, while the upper low-Ti lavas are deposited on the flanks, outside the dike injection zone, and therefore cut by almost no dikes at all (Fig. 2A).

core (Fig. 2A) correlate with the inferences drawn from the chemical subdivision. The low-Ti sequence (0–515 m) correlates with a very low dike fraction of only a few percent; the high-Ti sequence (665–1200 m) correlates with a high dike fraction of ca 50%; and the transition zone between the two sequences (515–665 m) correlates with dike abundance of a few tens of percent. The distribution of dikes in CY-1/1A then indicates that the low-Ti lavas solidified mostly outside the zone of dike injection whereas the high-Ti lavas solidified mostly inside that zone (see Fig. 3). The intermediate dike abundance of a few tens of percent in the transition zone suggests that the zone of inter-fingering high-Ti and low-Ti lava flows was located at the outer edges of the dike injection zone.

The shape and length scale of lava deposition in the Troodos spreading center (Fig. 4C) have been estimated by Schouten and Denham [22] using the post-depositional rotation of the paleomagnetic vectors in the CY-1/1A drill core. This length scale is a maximum estimate that can be shortened, particularly in the part of the distribution closest to the axis, but the basic shape remains the same. The basic shape is that of a bimodal distribution with a proximal mode $\ll$1000 m distance from the axis for the high-Ti sequence and a separate distal mode at $\sim$1500–2500 m distance for the low-Ti sequence. The lava deposition minimum at $\sim$1000–1500 m distance in Fig. 4C is dictated by the low post-depositional rotation angles in the chemical transition at 515–665 m composite depth in the core (Fig. 4A). Fig. 4C shows that most of the high-Ti lavas were deposited $<$1 km from the axis whereas the low-Ti lavas accumulated separately in a depocenter at approximately 2 km from the axis.

Baragar et al. [10] observe that the high- and low-Ti dikes in the Troodos sheeted complex and in CCSP Hole CY-4 have no preferred age relationship so that both types of dikes were injected penecontemporaneously and in close proximity along the spreading center. The chemical stratification of the Troodos lava pile shows that the low-Ti lavas were mostly deposited on top of the high-Ti lavas, implying that the low-Ti lavas were mostly deposited farther from the eruption center than the high-Ti lavas. If the deposition of high- and low-Ti lava was not spatially separated, or, if the spreading center changed location (jumped) on the scale of the lava deposition width, then high- and low-Ti lavas would be alternating throughout the Troodos volcanic sequence and there would be no correlation with dike fraction. Only a few samples of lavas with low-Ti characteristics are found in the deeper high-Ti

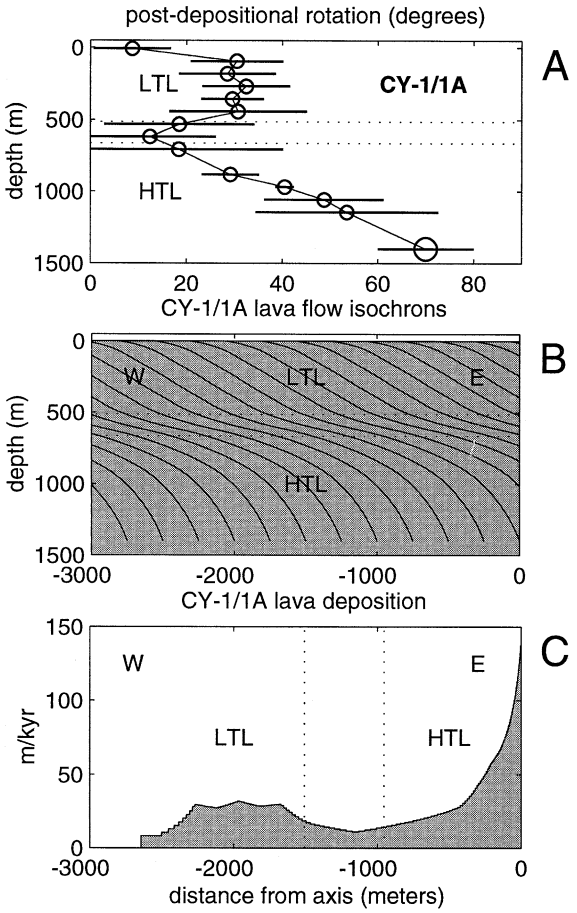

Fig. 4. Post-depositional rotation due to lava loading, isochrons, and lava deposition distribution in CY-1/1A (after [22]). (A) Post-depositional rotation derived from the averaged rotation of paleomagnetic vectors in CY-1/1A core samples (small open circles with 1σ error bars) and field observation (larger open circle at 1400 m). The rotations have been corrected for a 20° westward block rotation and a 20° northward rotation associated with the emplacement of the ophiolite. Dashed lines bound the transition from low-Ti lavas (LTL) to high-Ti lavas (HTL). (B) Isochron structure of the lava pile surrounding CY-1/1A, assuming isochrons were horizontal when the lava acquired its magnetization and lava loading was accommodated only by rotation about a horizontal axis. Dip of isochrons matches averaged post-depositional rotation in A. (C) Lava deposition distribution assuming dike-in-dike injection (i.e. C equals horizontal derivative of isochrons in B). Note that this distribution correlates with lava chemistry.

lava section in CY-1/1A (Fig. 2B) and in the deeper part of the Troodos lava pile [11,20]. This indicates how efficiently the low-Ti lava must have been transported away from the high-Ti lava depocenter at the axis. We infer that the rare occurrence of low-Ti lavas in the deeper high-Ti lava sequence indicates efficient transport of the low-Ti lavas away from the (proximal) high-Ti lava depocenter (i.e. virtually no deposition of low-Ti lavas near the axial eruption center) and a relative stability of the spreading axis.

Thus far we have used chemistry, dike abundance, and post-depositional deformation in the CY-1/1A core to specify the lava deposition environment at the Troodos paleo-spreading center. The high-Ti lavas were deposited near their eruption site on-axis and rapidly buried by later high-Ti lavas to become the deeper part of the lava pile. The low-Ti lavas, which also were erupted on-axis, were mostly deposited off-axis on the upper flanks of the ridge and became the shallow part of the lava pile.

To address the apparent paradox that low- and high-Ti lavas erupted together but were deposited separately, we calculate physical properties based on major element chemistry of the Troodos lavas in the CY-1/1A drill core.

4. Viscosity of the CY-1/1A lavas

Melt viscosities were calculated for reported rock compositions from the CY-1/1A drill holes, using the method of Shaw [23] (Fig. 5). We did not use more complex formulations which include the effects of crystallinity (e.g. [24]) because the crystal content during volcanic flow for the CY-1/1A lavas is not known. In order to make these calculations, pressure, melt composition, temperature, and water contents of melts must be estimated. The methods used to estimate each of these values are discussed below.

An eruptive pressure of 0.05 MPa was assumed for all lavas; the results of the calculations are insensitive to pressure variation from 0.01 to 0.1 MPa.

Melt composition was taken to be the volatile-free total of major element oxides analyzed in

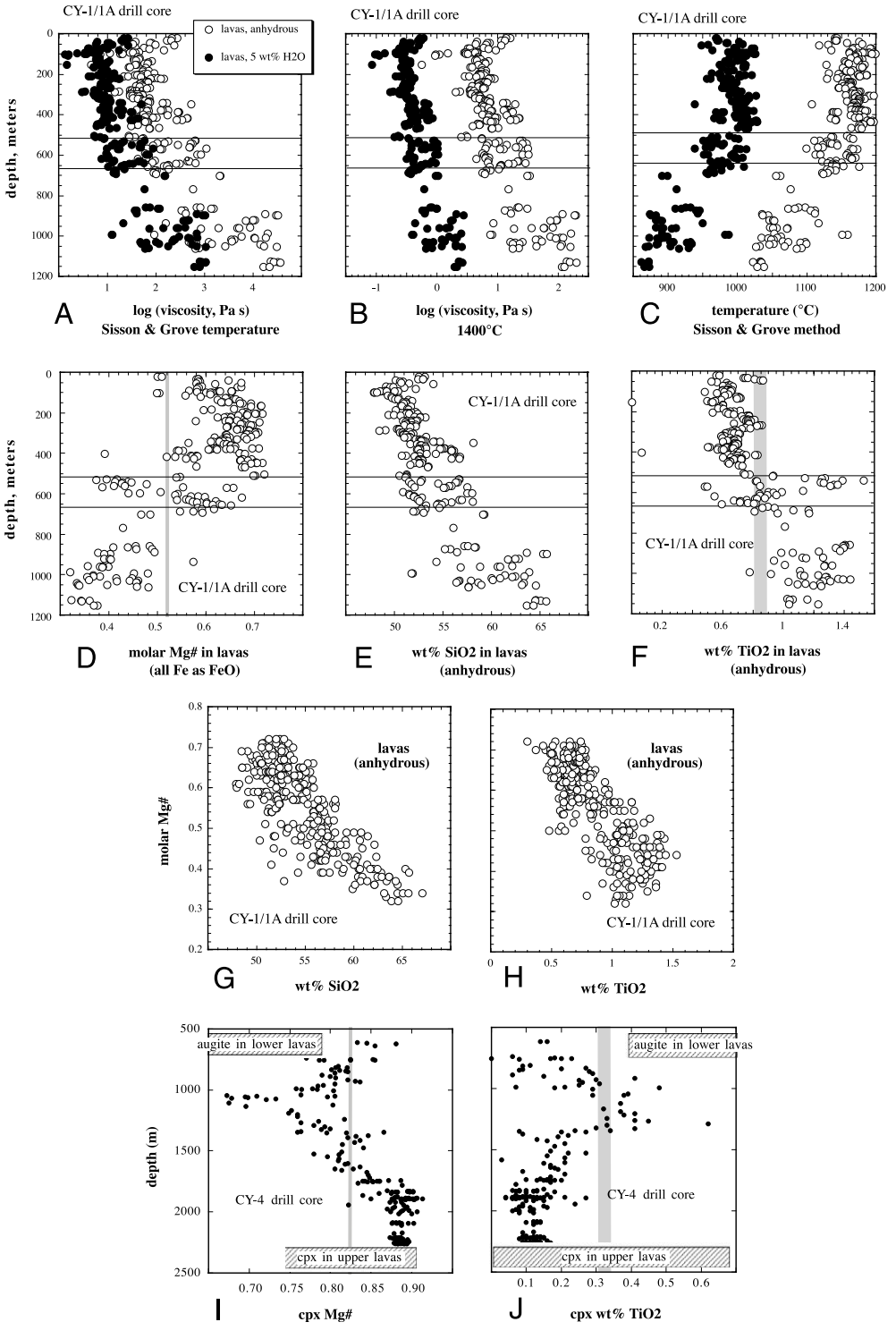
CY-1/1A drill core
lavas, anhydrous
lavas, 5 wt% H2O
depth, meters
A
log (viscosity, Pa s)
Sisson & Grove temperature
B
log (viscosity, Pa s)
1400°C
C
temperature (°C)
Sisson & Grove method
D
molar Mg# in lavas
(all Fe as FeO)
E
wt% SiO2 in lavas
(anhydrous)
F
wt% TiO2 in lavas
(anhydrous)
lavas
(anhydrous)
molar Mg#
G
wt% SiO2
H
wt% TiO2
depth (m)
augite in lower lavas
CY-4 drill core
cpx in upper lavas
I
cpx Mg#
J
cpx wt% TiO2

each sample plus, for the hydrous calculations, a controlled proportion of H_2O. This method implicitly assumes that all rocks represent aphyric lava compositions whose major element proportions were not modified by alteration. Neither of these assumptions is warranted for all samples. Very high MgO contents and Mg# (up to 24 wt% on an anhydrous basis, with molar Mg/(Mg+Fe) > 0.85) suggest the presence of accumulated olivine phenocrysts in some rocks. On the other hand Sobolev and co-workers [25] have argued that high MgO, high-temperature liquids were indeed an important lava type in Cyprus. We adopt a maximum cutoff at an Mg# of 0.73 which eliminates all outliers on a plot of MgO vs Mg#. The resulting trend closely resembles a liquid line of descent without accumulated olivine.

Similarly, much of the CY-1/1A core is highly altered. This is reflected in the whole rock analyses, which include maximum values of H_2O^+, loss on ignition, CO_2 and S of 9.1, 8.8, 20.1 and 1.3 wt%, respectively, and a minimum oxide total of 71.6 wt% (not all labs analyzed for volatile components). In this study, we chose a minimum cutoff of 90 wt% for the total of all volatile-free, major element oxides. Combination of this cutoff with the Mg# filter described in the previous paragraph results in acceptance of 78% of the reported analyses from the CY-1/1A core. Raising the cutoff to 95 wt% reduces the proportion of acceptable values to 37%, which we considered too small.

The overall effect of alteration on the anhydrous lava compositions in Cyprus has been a controversial topic (e.g. [4,5,7,8]), but the discovery of glasses with compositions comparable to Cyprus lava whole rock compositions [6] has reduced the uncertainty associated with this question. Relative to their fresh precursors, the CY-1/1A lavas are enriched in K_2O (up to 5 wt%) and depleted in Na_2O (up to 1 wt%); depleted or enriched in CaO (±6 wt%) (depending on carbonate content); and locally SiO_2-depleted (up to 2 wt%) and MgO-enriched [26]. These trends are most pronounced in the low-Ti suite (i.e. upper pervasive oxidized zone).

←

Fig. 5. Results of calculations using major element data for the CY-1/1A drill core as reported in Gibson et al. [17], with modifications as discussed in the text. A–C show hydrous and anhydrous melt viscosities and temperatures for rock composition vs composite depth in Holes CY-1 and CY-1A. Lines at 515 and 665 m bracket the transition zone between low-Ti lavas above to high-Ti lavas below. (A) Viscosities at magmatic temperatures from C. (B) Viscosities at 1400°C. (C) Magmatic temperatures using the liquid thermometer of Sisson and Grove [27]. There is a general increase of melt viscosity with depth related to rock composition; the similarity between A and B shows that this is not an artifact introduced by the temperature estimation method. D–F show molar Mg# (molar Mg/(Mg+Fe)), SiO_2 and TiO_2 vs depth in Holes CY-1 and CY-1A. There is a systematic variation in TiO_2, SiO_2 and Mg#, ranging from high-Ti dacites with 65 wt% SiO_2 and low Mg# in the lower lavas to low-Ti basalts with 50 wt% SiO_2 and high Mg# in the upper lavas. Variable SiO_2 is the main cause of the calculated viscosity variation in A and B. Shaded vertical lines at a molar Mg# of 0.52 and at 0.85 wt% TiO_2 separate upper and lower lavas. G and H show SiO_2 and TiO_2 vs Mg# in lavas from CY-1 and CY-1A drill cores. SiO_2, TiO_2, and Mg# variation are correlated and show that the rocks range from primitive basalt to evolved dacites. Despite suggestions that most Cyprus lavas fall into two, genetically distinct liquid lines of descent [6,10,15,32], the compositional trends of the lavas in G and H form a single group. For example, there are not two distinct trends in the plot of TiO_2 vs Mg# in H. I and J show clinopyroxene Mg# and TiO_2 content vs depth in plutonic rocks from CCSP Hole CY-4. Shaded vertical lines at 0.825 cpx Mg# and 0.32 cpx wt% TiO_2 are calculated from liquid compositions indicated with the shaded vertical lines which separate the upper and lower lavas in D and F (using a clinopyroxene/liquid Fe/Mg K_d of 0.23 – e.g. [39], figure 3 – and a clinopyroxene/liquid Ti K_d of 0.38 from [43]). Lower crustal cumulates, at greater than 1700 m depth in the hole, have clinopyroxenes with Mg# greater than 0.825 and TiO_2 less than 0.32 wt%, consistent with crystallization from primitive basalts with Mg#'s greater than 0.52 and TiO_2 less than 0.85 wt%, such as those found in the upper lavas of the CY-1/1A section. In contrast, mid-crustal gabbroic rocks sampled from 700 to 1700 m depth in the CY-4 hole have clinopyroxenes with Mg#'s from 0.65 to 0.825 and TiO_2 greater than 0.32 wt%, consistent with crystallization from more evolved liquids with Mg#'s from 0.3 to 0.52 and TiO_2 greater than 0.85 wt%, such as the lavas in the lower part of the CY-1A core. Such a correlation has previously been suggested by several investigators [42,44,45] on the basis of TiO_2 contents in clinopyroxene in Hole CY-4 (compare J and F). This is also reflected in the direct comparison of clinopyroxene compositions. Hachured boxes show a range of composition of clinopyroxene phenocrysts in lower lavas (augites in HTS of [13]) and upper lavas (clinopyroxene in LTS but not Lo-LTS of [13]). Only upper lavas have clinopyroxene phenocrysts with Mg# as high and TiO_2 contents as low as clinopyroxene in plutonic rocks at greater than 1700 m in Hole CY-4.

Net enrichment of the lavas in K_2O and depletion in Na_2O would affect their calculated viscosity in opposite ways. If lavas were originally poor in K but had the same Na contents, the true viscosities would have been higher than the calculated ones using the observed K_2O contents. Conversely, if lavas were originally rich in Na compared to their post-alteration compositions, then the true viscosities would have been lower than the calculated ones. We can determine upper bounds for the difference between the true and calculated viscosities by assuming that all the K_2O observed in upper lavas was added by alteration, while all the Na_2O was in the original composition prior to alteration. This should yield the highest possible estimate for the true viscosity prior to alkali metasomatism. Viscosities for the CY-1/1A lavas calculated without K_2O differ by less than 1.6 Pa s from those calculated with observed K_2O contents. This difference is negligible in the context of our paper.

If low SiO_2 lavas, mainly in the upper part of the volcanic section, preferentially lost SiO_2, while high SiO_2 lavas, mainly in the lower part of the volcanic section, did not lose SiO_2, this would diminish the viscosity contrast between the upper and lower lavas. To estimate the magnitude of this effect, we added 2 wt% SiO_2 to all lavas with less than 53 wt% SiO_2, and recalculated viscosities again. This should provide a maximum bound on the effect of metasomatic SiO_2 depletion. In this case, the higher SiO_2 viscosities differ from those calculated with observed SiO_2 contents by less than 2.2 Pa s. Again, this is not a significant effect in the context of our paper.

In our calculation of melt viscosities (Fig. 5A,B), two temperature values were used: (1) 1400°C, well above the liquidus temperature of most or all of the CY-1/1A lava compositions, and (2) temperature calculated using the liquid thermometer of Sisson and Grove [27] (Fig. 5C). The latter method is, in principle, better for determining the true viscosity of the lavas. However, the Sisson and Grove method for estimating magmatic temperature requires the assumption that melts are multiply saturated with olivine+plagioclase+clinopyroxene. For anhydrous crystallization of basalt, most lava compositions with less than 10 wt% MgO will be saturated in olivine+plagioclase+clinopyroxene (e.g. [28], figure 3; [29], figure 1). Although many Cyprus lavas contain relatively high MgO compared to, e.g., mid-ocean ridge basalts, only 12% of our filtered dataset has more than 10 wt% MgO (on an anhydrous basis) with a maximum value of 12.9 wt%.

In the Troodos ophiolite, which may have formed in a supra-subduction zone environment (e.g. [6,30]), primary 'arc' and 'boninitic' lavas may have included significant magmatic H_2O. The Sisson and Grove method is useful in such settings, because it explicitly accounts for the effect of H_2O on magmatic temperature. However, hydrous, primitive melts at lower crustal pressures during formation of the Troodos ophiolite probably were not saturated in plagioclase, as is reflected in the absence of plagioclase from olivine+clinopyroxene cumulates in the lower part of the CY-4 drill hole. Nevertheless, on the seafloor at a pressure of, e.g., 0.05 GPa, initially high magmatic H_2O would have rapidly degassed, leading to olivine+plagioclase+clinopyroxene saturation in lavas with less than 10 wt% MgO. For these reasons, we think that most Troodos lavas were probably multiply saturated with olivine+plagioclase+clinopyroxene, and therefore the Sisson and Grove method is appropriate for estimating magmatic temperature.

Open circles in Fig. 5A,B show calculated melt viscosities for anhydrous (0% H_2O) CY-1/1A rock compositions. It is clear that there is a substantial downhole increase in melt viscosity. While this gradient is clearer for the plots in which we have used estimated magmatic temperature (Fig. 5A), it is also apparent in the plot where a constant melt temperature of 1400°C was used (Fig. 5B). Thus, the relative downhole variation in melt viscosity is a result of varying rock composition, and not an artifact introduced by the temperature estimation method.

It is thought that Cyprus lavas were produced in a supra-subduction zone environment, and so primary, mantle-derived magmas may have contained substantial H_2O. Dissolved H_2O dramatically reduces melt viscosity, so we also estimated viscosities for hydrous melts. To do this, we added 5 wt% H_2O to each CY-1/1A rock compo-

sition, and then recalculated melt temperatures and viscosities. This is a substantial overestimate of the amount of water that can be dissolved in magmas at seafloor pressures. In fact, Muenow et al. [31] found 2–3 wt% in Troodos glass, and inferred that it was partially degassed during or after eruption. Thus, the hydrous viscosity estimates (filled circles in Fig. 5A–C) can be taken as minimum values, whereas in this context the anhydrous viscosity estimates (open circles in Fig. 5A–C) are maximum values.

As expected, the hydrous viscosity estimates are more than a factor of 10 lower than the anhydrous estimates. Both hydrous and anhydrous estimates show a downhole increase in viscosity. It is possible that the high-viscosity lavas in the lower part of the hole had substantially higher eruptive H_2O contents than the lower viscosity lavas in the upper part of the hole. If so, then the viscosity differences between the lower and upper lavas could have been smaller. However, the hydrous viscosities for the lower lavas are higher than the anhydrous viscosities for most of the upper lavas, so even in the extreme case in which lower lavas were H_2O-oversaturated while upper lavas were completely anhydrous, melt viscosities increase downhole.

5. Discussion

5.1. Down-section variation in lava composition

As stated earlier, the downhole increase in viscosity is primarily caused by complementary compositional gradients. These are shown in Fig. 5D–F. In addition to the well known division of lavas into high-Ti lower lavas and low-Ti upper lavas (Fig. 5F), Fig. 5D,E illustrates the systematic variation in SiO_2 and Mg#, ranging from dacites with 65 wt% SiO_2 and low Mg# in the lower lavas to basalts with 50 wt% SiO_2 and high Mg# in the upper lavas. Variable SiO_2 is the main cause of the calculated viscosity variation in Fig. 5A,B.

SiO_2, TiO_2, and Mg# variations in CY-1/1A rocks are correlated (Fig. 5G,H), and show that the rocks range continuously from primitive basalt to evolved dacites. Furthermore, despite suggestions that most Cyprus lavas fall into two, genetically distinct liquid lines of descent (e.g. [6,10,13–15,32]), the compositional trends of the lavas in Fig. 5G,H form a single group. For example, there are not two distinct trends in the plot of TiO_2 vs Mg# (Fig. 5H). Observed variation in TiO_2 at a given Mg# may indeed be due to mixing of melts derived from two distinct primary liquids, but to first order the rock compositions from CY-1/1A might be regarded as a single liquid line of descent. This observation surprised us, given past emphasis on the presence of distinct 'tholeiitic' and 'depleted' or 'boninitic' magmatic suites. However, the apparent discrepancy on this point is not of central importance in the present discussion.

5.2. Down-section variation in lava temperature

Given that there are more evolved lavas at the base and more primitive lavas at the top of the CY-1/1A section, it should come as no surprise that the temperatures estimated using the Sisson and Grove [37] method suggest a systematic downhole decrease in magmatic temperature (Fig. 5C). The median magmatic temperature of the low-Ti lavas (<515 m) is $\sim$125°C higher than that of the high-Ti lavas (>665 m). A gradient from more evolved, colder magmas at the bottom of the hole to more primitive, hotter magmas at the top apparently is not consistent with a scenario in which younger, off-axis lavas are emplaced above older, on-axis lavas. Instead, one would expect off-axis lavas to be colder and more evolved, since they must pass through a thick conductive boundary layer between the partially molten mantle and the seafloor. Instead, the systematic downhole variation in melt composition and temperature is consistent with a scenario in which all lavas were erupted on-axis, but the hotter, primitive lavas flowed farther off-axis than the colder, evolved lavas.

5.3. Depth of magma reservoirs in the crust

Penecontemporaneous eruption of evolved and primitive lavas requires spatially distinct magma

reservoirs to feed compositionally distinct lava flows. Baragar et al. [10] postulated discrete reservoirs distributed along the spreading axis with dikes extending vertically and longitudinally in the spreading plane and interleaving at depth to form a sheeted dike zone of varied provenance. Another option is that hotter, primitive lavas were fed from magma reservoirs near the base of the crust, while colder, more evolved lavas were fed from shallow melt reservoirs. Such an idea is consistent with the hypothesis that at least two melt reservoirs are present at different depths beneath the axes of some mid-ocean ridges, one at 1–3 km below the seafloor, and another near the base of the igneous crust [29,33–40].

We find support for this hypothesis in the drill core data of Hole CY-4, located ca 15 km SSW of Holes CY-1/1A (Fig. 1), which sampled much of the plutonic section of the Troodos ophiolite [41,42]. There is a systematic downhole variation in Mg# and TiO_2 of cumulate gabbros and pyroxenites in the middle and lower crustal section sampled by this hole (Fig. 5I,J). Lower crustal pyroxenites, at greater than 1700 m depth in the hole, have clinopyroxenes with Mg# greater than 0.825 and TiO_2 less than 0.32 wt%, consistent with crystallization from primitive basalts with Mg#'s greater than 0.52 and TiO_2 less than 0.85 wt%, such as those found in the upper lavas of the CY-1/1A section. In contrast, mid-crustal gabbroic rocks sampled from 700 to 1700 m depth in the CY-4 hole have clinopyroxenes with Mg#'s from 0.65 to 0.825 and TiO_2 greater than 0.32 wt%, consistent with crystallization from more evolved liquids with Mg#'s from 0.3 to 0.52 and TiO_2 greater than 0.85 wt%, such as the lavas in the lower part of the CY-1A core. Such a correlation has previously been suggested by several investigators [13,42,44,45] on the basis of Mg# and TiO_2 contents in clinopyroxene in the CY-4 drill core, in comparison with whole rock and clinopyroxene phenocryst compositions in the lavas (Fig. 5J). Clinopyroxene compositions indicated with shaded vertical lines at 0.825 Mg# and 0.32 wt% TiO_2 in Fig. 5I,J are consistent with the liquid compositions separating upper and lower lavas indicated with shaded vertical lines in Fig. 5D,F (using a clinopyroxene/liquid Fe/Mg K_d of 0.23 (e.g. [39], figure 3) and a clinopyroxene/liquid Ti K_d of 0.38 from [40]).

5.4. Down-section variation in viscosity

The systematic increase of lava viscosity, over several orders of magnitude, with depth in the Troodos lava pile suggests that lava segregation by viscosity would provide a mechanism for its chemical stratification. The velocity of a body of fluid on an inclined plane is inversely related to its viscosity [46]. The lower viscosity, low-Ti lavas flowed faster and farther down the upper slopes of the paleo Troodos Rise than the higher viscosity high-Ti lavas. The lowest viscosity lavas traveled farthest from the axis and became the top of the lava pile, whereas the highest viscosity lavas traveled least, were buried deepest by later high-viscosity lavas, and became the bottom of the lava pile. High-Ti lavas with the lowest viscosity traveled farthest from the axis to inter-finger with low-Ti lavas of the same viscosity in the chemical transition zone (515–665 m). The low magmatic viscosity of 10^{1-2} Pa s in the shallow lavas is the viscosity of warm corn syrup; the high viscosity of 10^{3-4} Pa s in the deeper lavas is the viscosity of cold honey. The eruption viscosity will be higher than the melt viscosity because of crystallinity and cooling during transit of the magmas to the seafloor.

The down-slope distance traveled by a body of lava also depends on its volume. A small volume cools faster and will not go as far. Baragar et al. [10] report that only 20% of the sampled Troodos dikes belong to the low-Ti suite. In CY-1/1A, low-Ti lavas are 1.5 times more voluminous than high-Ti lavas. If the low- and high-Ti dikes have the same length along the axis and the same width, this implies that the volume of low-Ti lavas erupted per dike event was six times larger than that of the high-Ti lavas. However, the thickness of the low-Ti lavas in Holes CY-1/1A is not typical of the area. Bednarz and Schmincke [13] estimate that one third of the volcanic pile and $\sim$15% of the dike section are composed of low-Ti lithologies. This implies the average volume of low-Ti lavas per dike event was three times larger than the average volume of high-Ti lavas per dike

event. The larger volume of low-Ti lavas erupted per dike event suggests that the segregation of the Troodos lavas was not only by viscosity but also by eruption volume.

Using the isochrons in Fig. 4B, which relate depth in the core to distance from the spreading center, we plot the lava viscosities in CY-1/1A against distance from point of eruption in Fig. 6. This shows that the distance that a packet of Troodos lava traveled away from its eruption center is related to its viscosity to the −1/2 to −1/3 power. The rare sample of low-viscosity lava at a closer distance (deeper level in the core) indicates this relation should be modeled as a packet of molten lava – a finite volume and not a constant stream – flowing down a sloping plane. Fig. 6 illustrates again how effective the transport of the low-viscosity lava was, since it hardly left a trace over a few hundred to 1000 m from the on-axis eruption center to the off-axis depocenter. Effective transport can occur in lava tubes or channels, which occupy only a small fraction of the length of the axis. Consequently, their proportion among on-axis lavas will be small.

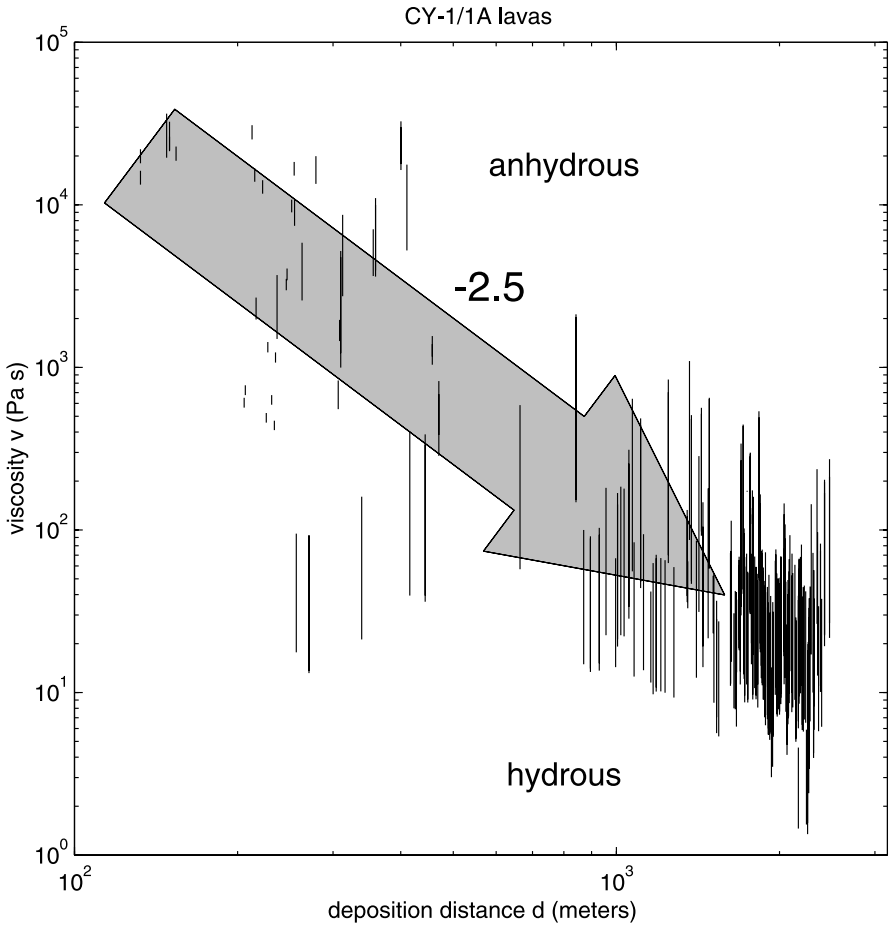

Fig. 6. Lava viscosity in CY-1/1A against horizontal distance from point of eruption, using the isochrons in Fig. 4B, which relate depth in the core to distance from the spreading center axis. Vertical bars show viscosity range for H_2O content of 0 wt% (upper limit of vertical bars) to 5 wt% (lower limit of vertical bars). The negative trend of the data shows that the distance a pocket of Troodos lava traveled away from its eruption center is inversely related to its viscosity. Note that the viscosity decrease with increasing distance from point of eruption cannot be accounted for by water content alone.

5.5. Melt transport from crustal reservoirs to the seafloor

The estimates of frequency and volume of the low- and high-Ti eruptions from the previous section further constrain the nature of melt transport for the upper and lower lavas in the Troodos ophiolite. It follows that eruptions of the low-Ti, high-temperature, primitive magmas from deep magma chambers were infrequent and voluminous, while eruptions of high-Ti, evolved magmas from shallow magma chambers were frequent but comparatively small.

6. Summary and conclusion

Viscosity at magmatic temperature calculated from major element composition of lava in CCSP Holes CY-1 and CY-1A increases systematically with depth in the Troodos lava pile. This viscosity ranges from 10^{1-2} Pa s (viscosity of warm corn syrup) in the shallow lavas to 10^{3-4} Pa s (viscosity of cold honey) in the deepest lavas in CY-1/1A. This suggests that Troodos lava deposition was controlled primarily by viscosity, with the least viscous lavas flowing and accumulating farthest from the axial eruption center and the most viscous lavas accumulating near the axis.

In addition, a clear though hypothetical picture of the transport of crustal melt in the Troodos ophiolite emerges from this work (Fig. 7). Primitive, low-viscosity upper lavas were fed via rare, voluminous eruptions from deep-crustal axial magma chambers. In the deep magma chambers, these melts formed ultramafic cumulates with Mg#'s greater than 0.825 by partial crystallization at high temperature. After rapid transport to the surface, probably in cracks, these low-viscosity magmas flowed for long distances away from the ridge axis, so that they are primarily preserved in the upper part of the volcanic section. Evolved viscous lower lavas were fed penecontemporaneously via frequent small-volume eruptions from shallower, mid-crustal axial magma chambers. In the mid-crustal magma reservoirs, melts formed gabbroic cumulates with Mg#'s less than 0.825 by partial crystallization at relatively low temperature. After transport to the surface, the eruptions of high-viscosity lavas were confined mainly to the axial rift or valley, and so are preserved mainly in the lower part of the volcanic section. Thus, the stratigraphic organization of Troodos upper and lower lavas probably has its origin in the presence of deep and shallow axial magma chambers which formed in a significant temperature gradient extending to the base of the crust.

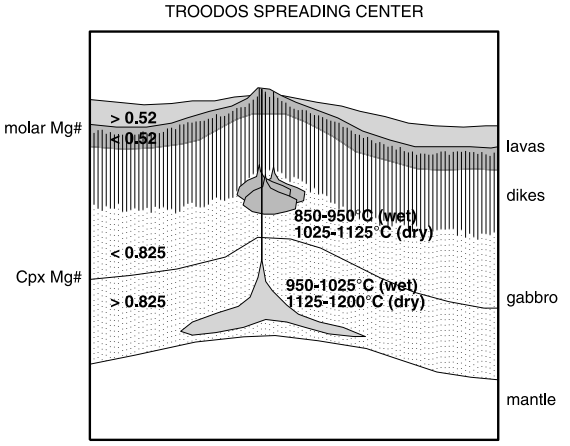

Fig. 7. Cartoon of the Troodos spreading center which illustrates how the shallow high-Ti lavas with higher Mg# came from high-temperature, lower crustal axial magma reservoirs that are now represented by high-Mg# pyroxenite cumulates, while the deeper low-Ti lavas with lower Mg# were erupted from lower-temperature, mid-crustal axial reservoirs that are now represented by gabbroic cumulates with lower Mg#.

Acknowledgements

This paper was greatly improved by helpful, informative reviews by Kathy Gillis and Philippe Pézard. H.S. was supported by National Science Foundation Grants OCE-9419472 and OCE-9819261 and the Woods Hole Oceanographic Institution. P.B.K. was supported by NSF Grants OCE-9416616, OCE-9711170, and OCE-9819666. H.S. especially thanks Joe Cann, Kathy Gillis, and Costas Xenophontos for introducing him to the Troodos ophiolite and providing guidance. We acknowledge Henry Dick and the W.M. Keck Foundation for supporting the stimulating interdisciplinary environment of the W.M. Keck Geodynamics Program at WHOI. We also wish to

acknowledge John Collins, Dan Fornari, Susan Humphris, Philippe Pézard, Maurice Tivey, and Jack Whitehead for helpful discussions. H.S. thanks Victoria Kaharl for editorial help with an early version of the manuscript. WHOI Contribution No. 10,617.*[BOYLE]*

References

[1] L.M. Bear, The geology and mineral resources of the Akaki-Lythrodondha area, Cyprus Geological Survey Memoir 3, 1960, 122 pp.

[2] R.A.M. Wilson, F.T. Ingham, The geology of the Xeros–Troodos area with an account of the mineral resources, Cyprus Geological Survey Memoir 1, 1959, 184 pp.

[3] J.H. Carr, L.M. Bear, The geology and mineral resources of the Peristerona–Lagoudhera area, Cyprus Geological Survey Memoir 2, 1960, 79 pp.

[4] I.G. Gass, J.D. Smewing, Intrusion, extrusion, and metamorphism at constructive margins evidence from the Troodos massif, Cyprus, Nature 242 (1973) 26–29.

[5] J.D. Smewing, K.O. Simonian, I.G. Gass, Metabasalts from the Troodos massif, Cyprus: genetic implications deduced from petrology and trace element geochemistry, Contrib. Mineral. Petrol. 51 (1975) 49–64.

[6] P.T. Robinson, W.G. Melson, T. O'Hearn, H.-U. Schmincke, Volcanic glass compositions of the Troodos ophiolite, Cyprus, Geology 11 (1983) 400–404.

[7] K.M. Gillis, P.T. Robinson, Low temperature alteration of the extrusive sequence, Troodos ophiolite, Cyprus, Can. Mineral. 23 (1985) 431–441.

[8] K.M. Gillis, Multistage alteration of the extrusive sequence, Troodos ophiolite, Cyprus, Ph.D. Thesis, Dalhousie University, Halifax, 1987, 387 pp.

[9] J. Malpas, D. Williams, Geology of the area surrounding the CY-1 and CY-1A boreholes, in: I.L. Gibson, J. Malpas, P.T. Robinson, C. Xenophontos (Eds.), Cyprus Crustal Study Project: Initial Report, Holes CY-1 and 1A, Geological Survey of Canada Paper 90-20, 1991, pp. 29–39.

[10] W.R.A. Baragar, M.B. Lambert, N. Baglow, I.L. Gibson, The sheeted dyke zone in the Troodos ophiolite, in: J. Malpas, E.M. Moores, A. Panayiotou, C. Xenophontos (Eds.), Ophiolites-oceanic crustal analogues, Proceedings of the Symposium 'Troodos 1987', Geological Survey Department, Nicosia, Cyprus, 1990, pp. 37–51.

[11] R.N. Taylor, Geochemical stratigraphy of the Troodos extrusive sequence: temporal developments of a spreading centre magma chamber, in: J. Malpas, E.M. Moores, A. Panayiotou, C. Xenophontos (Eds.), Ophiolites-oceanic crustal analogues, Proceedings of the Symposium 'Troodos 1987', Geological Survey Department, Nicosia, Cyprus, 1990, pp. 173–183.

[12] J. Malpas, P.T. Robinson, Geology and geophysics of boreholes CY-1 and CY-1A of the Cyprus Crustal Drilling Project: Summary, in: I.L. Gibson, J. Malpas, P.T. Robinson, C. Xenophontos (Eds.), Cyprus Crustal Study Project: Initial Report, Holes CY-1 and 1A, Geological Survey of Canada Paper 90-20, 1991, pp. 255–261.

[13] U. Bednarz, H.-U. Schmincke, Petrological and chemical evolution of the northeastern Troodos Extrusive Series, Cyprus, J. Petrol. 35 (1994) 489–523.

[14] M.V. Portnyagin, L.V. Danyushevsky, V.S. Kamenetsky, Coexistence of two distinct mantle sources during formation of ophiolites; a case study of primitive pillow-lavas from the lowest part of the volcanic section of the Troodos Ophiolite, Cyprus, Contrib. Mineral. Petrol. 128 (1997) 287–301.

[15] J.M. Mehegan, Temporal, spatial, and chemical evolution of the Troodos ophiolite lavas, Cyprus: supra-subduction zone volcanism in the Tethis Sea, Ph.D. Thesis, Dalhousie University, Halifax, 1988, 700 pp.

[16] M.A. Lambert, R. Baragar, Part 2: Sheeted dikes of the Troodos ophiolite, in: C. Xenophontos, J.G. Malpas (Eds.), Field Excursion Guidebook, Troodos 87: Ophiolites and Oceanic Lithosphere, Geological Survey Department, Nicosia, Cyprus, 1987, pp. 142–157.

[17] I.L. Gibson, J. Malpas, P.T. Robinson, C. Xenophontos, Cyprus Crustal Study Project: Initial Report, Holes CY-1 and 1A, Geological Survey of Canada Paper 90-20, 1991, 283 pp.

[18] F.J. Vine, G.C. Smith, Structure and physical properties of the Troodos crustal section at ICRDG drill holes CY1, 1a and 4, in: J. Malpas, E.M. Moores, A. Panayiotou, C. Xenophontos (Eds.), Ophiolites-oceanic crustal analogues, Proceedings of the Symposium 'Troodos 1987', Geological Survey Department, Nicosia, Cyprus, 1990, pp. 113–124.

[19] J. Malpas, G. Barnable, Lithologic log of Holes CY-1 and CY-1A in: I.L. Gibson, J. Malpas, P.T. Robinson, C. Xenophontos (Eds.), Cyprus Crustal Study Project: Initial Report, Holes CY-1 and 1A, Geological Survey of Canada Paper 90-20, 1991, pp. 1–283.

[20] H.-U. Schmincke, U. Bednarz, Pillow, sheet flow and breccia flow volcanoes and volcano-tectonic hydrothermal cycles in the extrusive series of the northeastern Troodos ophiolite (Cyprus), in: J. Malpas, E.M. Moores, A. Panayiotou, C. Xenophontos (Eds.), Ophiolites-oceanic crustal analogues, Proceedings of the Symposium 'Troodos 1987', Geological Survey Department, Nicosia, Cyprus, 1990, pp. 185–206.

[21] P.A. Pézard, R.N. Anderson, W.B.F. Ryan, K. Becker, J.C. Alt, P. Gente, Accretion, structure and hydrology of intermediate spreading-rate oceanic crust from drillhole experiments and seafloor observations, Mar. Geophys. Res. 14 (1992) 93–123.

[22] H. Schouten, C.R. Denham, Comparison of volcanic construction in the Troodos ophiolite and oceanic crust using paleomagnetic inclinations from Cyprus Crustal Study Project (CCSP) CY-1 and CY-1A and Ocean Drilling Program (ODP) 504B drill cores, in: Y. Dilek, E. Moores,

D. Elthon, A. Nicholas (Eds.), Ophiolites and Oceanic Crust: New Insights from Field Studies and the Ocean Drilling Program, GSA Special Paper 349, 2000, pp. 181–194.
[23] H.R. Shaw, Viscosities of magmatic silicate liquids an empirical method of prediction, Am. J. Sci. 272 (1972) 870–893.
[24] H. Pinkerton, R.J. Stevenson, Methods of determining the rheological properties of magmas at sub-liquidus temperatures, J. Volcanol. Geotherm. Res. 53 (1992) 47–66.
[25] A.V. Sobolev, M.V. Portnyhagin, L.V. Dmitriev, O.P. Tsameryan, L.V. Danyushevsky, N.N. Kononkova, N. Shimizu, P.T. Robinson, Petrology of ultramafic lavas and associated rocks of the Troodos Massif, Cyprus, Petrology (translated from Petrologiya) 1 (1993) 331–361.
[26] U. Bednarz, H.-U. Schmincke, Mass transfer during subseafloor alteration of the upper Troodos crust (Cyprus), Contrib. Mineral. Petrol. 102 (1989) 91–101.
[27] T.W. Sisson, T.L. Grove, Temperatures and H_2O contents of low MgO high-alumina basalts, Contrib. Mineral. Petrol. 113 (1993) 167–184.
[28] J. Korenaga, P.B. Kelemen, Major element heterogeneity in the mantle source of the North Atlantic igneous province, Earth Planet. Sci. Lett. 184 (2000) 251–268.
[29] P.B. Kelemen, E. Aharonov, Periodic formation of magma fractures and generation of layered gabbros in the lower crust beneath oceanic spreading ridges, in: W.R. Buck, P.T. Delaney, J.A. Karson, Y. Lagabrielle (Eds.), Faulting and Magmatism at Mid-Ocean Ridges, American Geophysical Union, Geophysical Monograph 106, 1998, pp. 267–289.
[30] A. Miyashiro, The Troodos ophiolitic complex was probably formed in an island arc, Earth Planet. Sci. Lett. 19 (1973) 218–224.
[31] D.W. Muenow, M.O. Garcia, K.E. Aggrey, U. Bednarz, H.U. Schmincke, Volatiles in submarine glasses as a discriminant of tectonic origin; application to the Troodos Ophiolite, Nature 343 (1990) 159–161.
[32] J. Tarney, N.G. Marsh, Major and trace element geochemistry of Holes CY-1 and CY-4: Implications for petrogenetic models, in: I.L. Gibson, J. Malpas, P.T. Robinson, C. Xenophontos (Eds.), Cyprus Crustal Study Project: Initial Report, Holes CY-1 and 1A, Geological Survey of Canada Paper 90-20, 1991, pp. 133–175.
[33] J. Garmany, Accumulations of melt at the base of young oceanic crust, Nature 340 (1989) 628–632.
[34] J.H. Bédard, Cumulate recycling and crustal evolution in the Bay of Islands ophiolite, J. Geol. 99 (1991) 225–249.
[35] F. Boudier, A. Nicolas, Nature of the Moho Transition Zone in the Oman ophiolite, J. Petrol. 36 (1995) 777–796.
[36] F. Boudier, A. Nicolas, B. Ildefonse, Magma chambers in the Oman ophiolite: Fed from the top and the bottom, Earth Planet. Sci. Lett. 144 (1996) 239–250.
[37] R.A. Dunn, D.R. Toomey, Seismological evidence for three-dimensional melt migration beneath the East Pacific Rise, Nature 388 (1997) 259–262.
[38] P.B. Kelemen, K. Koga, N. Shimizu, Geochemistry of gabbro sills in the crust/mantle transition zone of the Oman ophiolite: Implications for the origin of the oceanic lower crust, Earth Planet. Sci. Lett. 146 (1997) 475–488.
[39] J. Korenaga, P.B. Kelemen, The origin of gabbro sills in the Moho transition zone of the Oman ophiolite: Implications for magma transport in the oceanic lower crust, J. Geophys. Res. 102 (1997) 27729–27749.
[40] W.C. Crawford, S.C. Webb, J.A. Hildebrand, Constraints on melt in the lower crustal and Moho at the East Pacific Rise, 9 degrees 48′N, using seafloor compliance measurements, J. Geophys. Res. 104 (1999) 2923–2939.
[41] P. Browning, S. Roberts, T. Alabaster, Fine-scale modal layering and cyclic units in ultramafic cumulates from the CY-4 borehole, Troodos ophiolite: Evidence for an open system magma chamber, in: I.L. Gibson, J. Malpas, P.T. Robinson, C. Xenophontos (Eds.), Cyprus Crustal Study Project: Initial Report, Hole CY-4, Geological Survey of Canada Paper 88-9, 1989, pp. 193–220.
[42] J. Malpas, T. Brace, S.M. Dunsworth, Structural and petrologic relationships of the CY-4 drill hole of the Cyprus Crustal Study Project, in: I.L. Gibson, J. Malpas, P.T. Robinson, C. Xenophontos (Eds.), Cyprus Crustal Study Project: Initial Report, Hole CY-4, Geological Survey of Canada Paper 88-9, 1989, pp. 39–67.
[43] S.R. Hart, T. Dunn, Experimental Cpx/melt partitioning of 24 trace elements, Contrib. Mineral. Petrol. 113 (1993) 1–8.
[44] P. Thy, Magmas and magma chamber evolution, Troodos ophiolite, Cyprus, Geology 15 (1987) 316–319.
[45] P. Thy, E.M. Moores, Crustal accretion and tectonic setting of the Troodos Ophiolite, Cyprus, Tectonophysics 147 (1988) 221–245.
[46] D.L. Turcotte, G. Shubert, Geodynamics, John Wiley and Sons, New York, 1982, 448 pp.
[47] H.-U. Schmincke, M. Rautenschlein, P.T. Robinson, J.M. Mehegan, Troodos extrusive series of Cyprus A comparison with oceanic crust, Geology 11 (1983) 405–409.
[48] J.M. Mehegan, P.T. Robinson, Lava groups and volcanic stratigraphy of the CCSP boreholes CY-1 and CY-1A, Troodos ophiolite, Cyprus, in: I.L. Gibson, J. Malpas, P.T. Robinson, C. Xenophontos (Eds.), Cyprus Crustal Study Project: Initial Report, Holes CY-1 and 1A, Geological Survey of Canada Paper 90-20, 1991, pp. 177–185.
[49] H.-U. Schmincke, M. Rautenschlein, Troodos extrusive series (Akaki River canyon) and the sheeted diabase, in: C. Xenophontos, J.G. Malpas (Eds.), Field Excursion Guidebook, Troodos 87: Ophiolites and Oceanic Lithosphere, Geological Survey Department, Nicosia, Cyprus, 1987, pp. 260–285.
[50] R.J. Varga, J.S. Gee, H. Staudigel, L. Tauxe, Dike surface lineations as magma flow indicators within sheeted dike complex of the Troodos Ophiolite, Cyprus, J. Geophys. Res. 103 (1998) 5241–5256.